JACS
JOURNAL OF THE AMERICAN CHEMICAL SOCIETY
Article
pubs.acs.org/JACS

# Understanding the Reactivity of $Pd^0/PR_3$-Catalyzed Intermolecular $C(sp^3)$–H Bond Arylation

Travis M. Figg,[†] Masayuki Wasa,[‡] Jin-Quan Yu,*[,‡] and Djamaladdin G. Musaev*[,†]

[†]Cherry L. Emerson Center for Scientific Computation, Emory University, 1515 Dickey Drive, Atlanta, Georgia 30322, United States
[‡]Department of Chemistry, The Scripps Research Institute, 10550 North Torrey Pines Road, La Jolla, California 92037, United States

Supporting Information

**ABSTRACT:** Mechanistic details pertaining to the $Pd^0/PCy_3$-catalyzed intermolecular arylation of a terminal $\beta$-$C(sp^3)$–H bond aryl amide substrate (**SM** = EtCONH-Ar, where Ar = $C_6H_5$, $C_6F_5$ and CONH-Ar is a directing group (**DG**)) in the presence of CsF base were elucidated. Key mechanistic features of this reaction are (1) oxidative addition of the aryl halide PhI to $Pd^0/PCy_3$, (2) deprotonation of **SM** by CsF to form **DG′** = [EtCON-Ar]$Cs^+$ for subsequent coordination to intermediate I–$Pd^{II}(PCy_3)$Ph (the substantially lower $pK_a$ of the $EtCONHC_6F_5$ in comparison to $EtCONHC_6H_5$ is instrumental for the presence of a larger population of the reactive deprotonated amides for Ar = $C_6F_5$), (3) "$Cs_2$–I–F" cluster formation upon external (the second) CsF molecule approach to the active site of the I–$Pd^{II}(PCy_3)$Ph(**DG′**) intermediate, (4) "$Cs_2$–I–F cluster" assisted $\beta$-$C(sp^3)$–H bond activation via a concerted metalation–deprotonation (CMD) mechanism, and (5) reprotonation of the amide directing group to facilitate the $C(sp^3)$–Ph reductive elimination. The energy barriers, $\Delta G^{\ddagger}$ ($\Delta G^{\ddagger}_{disp}$), associated with the "$Cs_2$–I–F cluster" mediated $\beta$-$C(sp^3)$–H bond activation transition state are 6.5 (8.7) and 10.2 (12.9) kcal/mol when **DG** = $CONHC_6H_5$, $CONHC_6F_5$, respectively. It was shown that (a) the $PCy_3$ ligand only semidissociates upon $\beta$-$C(sp^3)$–H bond cleavage and (b) the I-to-F substitution in I–[$Pd^{II}$](Ph)($PCy_3$)(**DG′**) is a facile process that makes the "direct-halide" assisted $\beta$-$C(sp^3)$–H bond activation relatively less energy demanding and opens the possibility for a competing Ph–F bond formation reaction. It was shown that the "direct-I" assisted C–H bond activation TS, which associates with a relatively large energy barrier, is an H-atom insertion transition state into the Pd–I bond, while the "direct-F" assisted C–H bond activation TS, which occurs with a relatively low energy barrier (but still is much larger than that required for the "$Cs_2$–I–F cluster" assisted pathway), is a direct proton abstraction transition state.

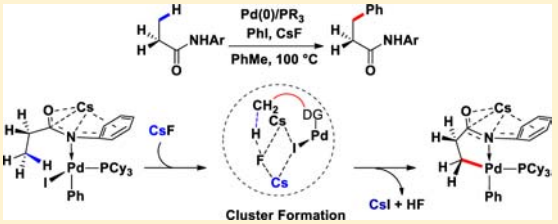


## I. INTRODUCTION

Selective C–H functionalization has been a longstanding challenge due to the inert and ubiquitous nature of the C–H bond. Therefore, the development of transition-metal catalysts that can facilitate selective C–H modification has occupied the minds of many scientists. Success in this field is expected to open overwhelming potential for a myriad of useful chemical transformations.[1] Extensive studies have shown Pd catalysts to be especially effective for a large number of C–H functionalization reactions, partially due to the diverse reactivity of the Pd–carbon bonds leading to a variety of carbon–carbon and carbon–heteroatom bonds.[1−5]

Among the various type of redox catalysis employed in Pd-catalyzed C–H functionalizations, including (but not limited to) $Pd^0/Pd^{II}$ and $Pd^{II}/Pd^{IV}$ catalysis,[2a] the $Pd^0/Pd^{II}$ manifold initiated by the oxidative addition of aryl halides has a unique advantage: no external oxidant is needed in this reaction. $Pd^0/PR_3$-catalyzed arylation of $C(sp^2)$–H bonds with aryl halides have been extensively reported since the 1970s.[2b] Pioneering works on $Pd^0/PR_3$-catalyzed intramolecular arylation of $C(sp^3)$–H bonds with a tethered aryl halides has also been reported.[4]

However, the proposed mechanistic model (Figure 1a), based on the reported *intramolecular* reactions, calls into question whether an analogous *intermolecular* $C(sp^3)$–H arylation is feasible.[6] Following the same mechanistic model, an *intermolecular* $C(sp^3)$–H activation using directed C–H activation (Figure 1b) would require an additional (i.e., fifth) coordination site to coordinate the directing group and about to be activated C–H bond.

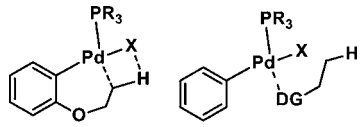


**Figure 1.** (a) Transition state for intramolecular $sp^3$ C–H arylation. (b) Precursor for intermolecular $sp^3$ C–H activation.

Intriguingly, Yu and co-workers have recently reported the first experimental example of the $Pd^0/PR_3$-catalyzed *intermo-*

**Received:** May 28, 2013
**Published:** September 4, 2013




dx.doi.org/10.1021/ja4053416 | J. Am. Chem. Soc. 2013, 135, 14206−14214

*lecular* selective terminal $\beta$-C($sp^3$)−H functionalization with aryl iodides (Scheme 1).[7] The reaction conditions (i.e., ligands, bases, solvents, and coupling partners) were screened to improve the yield for the desired monoarylated products.

**Scheme 1. Selective $\beta$-C($sp^3$)−H Bond Arylation using *N*-Aryl Amides in Conjunction with $Pd^0/PR_3$ Catalysts, PhI, and CsF**[a]

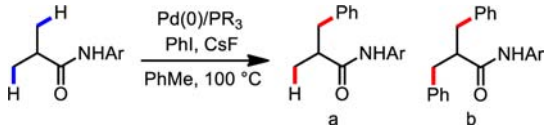


[a]Ar = $C_6F_5$. Adapted with permission from ref 7.

Bulky electron-rich $PR_3$ ligands such as $PCy_3$ and Buchwald ligands were found to be optimal. CsF is reported to be the most efficient base and gave appreciable amounts of the desired products. Interestingly, when $Cs_2CO_3$ was used, a diminished yield of the product was obtained for substrates containing $\alpha$-hydrogens; however, substrates that did not contain $\alpha$-hydrogens give arylated products in moderate yields. Additionally, only aryl iodides were found to give the desired product. Other aryl halides and pseudohalides such as aryl bromides, chlorides, triflates, and tosylates did not carry out the reaction. The substrate (**SM** = EtCONH-Ar), containing an aryl component (Ar = $C_6H_5$, $C_6F_5$), was found to greatly improve the reactivity when decorated with electron-withdrawing substituents. Overall, the desired $\beta$-C($sp^3$)−H arylation was found to be optimal when Ar = $C_6F_5$, $PR_3$ = Buchwald's cyclohexyl JohnPhos ligand, and base = CsF.[7]

However, the presented experimental results[7] raise several questions.

(1) In light of the requirement for the directing group **DG** (**DG** = CONHAr or its deprotonated derivative CONAr) to remain coordinated for the C−H bond cleavage, which would require an additional coordination site (Figure 1), an apparent question arises: does the directing group **DG** and/or $PR_3$ group dissociate in the course of the reaction? This event was a subject of recent discussion in the literature.[8]

(2) Why does placing electron-withdrawing substituents on the aryl component of the **DG** greatly improve the reactivity of the system? A better understanding of this phenomenon could lead to beneficial modifications on the directing group that, in turn, could result in the design of more efficient catalytic systems.

(3) Why is CsF the most efficient base for this reaction? Delineation of the role of base in C−H bond arylation is currently under debate.[9] Several computational studies, which focus on carbonate, bicarbonate, or acetate as the model for the base, suggest the base plays a crucial role in promoting C−H bond activation either through a concerted metalation−deprotonation (CMD) or a stepwise mechanism.[9,10]

Since the reaction reported by Yu (see Scheme 1) is a rare example of selective $\beta$-C($sp^3$)−H functionalization, a better understanding of the aforementioned key mechanistic implications could facilitate the design of more efficient catalysts that will expand the substrate scope of this important reaction. Therefore, herein, we report a joint computational and experimental study to shed light on the mechanistic aspects of the reaction outlined in Scheme 1. The results of this study will guide future experimental efforts in designing successful catalysts for the activation and subsequent arylation of C($sp^3$)−H bonds.

## II. COMPUTATIONAL PROCEDURES

Calculations were carried out using the Gaussian 09 suite of programs.[11] The geometries of all reported reactants, intermediates, transition states, and products were optimized without symmetry constraints at the M06-L level of density functional theory[12] in conjunction with the Lanl2dz basis set and corresponding Hay−Wadt effective core potential (ECP)[13] for Pd, I, and Cs. Standard 6-31G(d,p) basis sets were used for all remaining atoms (below we call this approach M06-L/{Lanl2dz+[6-31G(d,p)]} or M06-L/BS1).

The structure and energy of the important C($sp^3$)−H activation step for both substrate modifications for Ar = $C_6H_5$, $C_6F_5$ were improved by using larger basis sets with diffuse functions on light atoms, Lanl2dz+[6-31++G(d,p)] (below we call this basis set BS2). Several other density functionals such as M06, B3LYP, and B3LYP+D were also validated.

We briefly compare results obtained at the M06-L/BS1, M06-L/BS2, M06/BS2, B3LYP/BS2, and (B3LYP+D)/BS2 levels of theory. In general, the M06-L/BS1, M06-L/BS2, M06/BS2, and B3LYP/BS2 approaches provide very similar (within a few kcal/mol) difference in the C($sp^3$)−H activation barrier for Ar = $C_6H_5$, $C_6F_5$ (i.e., $\Delta G_{CMD}^{\ddagger}$[(Ar = $C_6H_5$) − (Ar = $C_6F_5$)]); see the Supporting Information for more details. However, inclusion of the Grimme dispersion correction slightly changes these values. The larger changes were found for the direct-F assisted C−H activation barriers (i.e., upon use of (B3LYP+D)/BS2):[14] in this case the M06-L/BS2 and (B3LYP+D)/BS2 calculated $\Delta G_{CMD}^{\ddagger}$[(Ar = $C_6H_5$) − (Ar = $C_6F_5$)] values are 14.3 and 4.3 kcal/mol, respectively. For the $Cs_2$−I−F cluster mediated transition states these methods show smaller differences: the M06-L/BS2 and (B3LYP+D)/BS2 calculated $\Delta G_{CMD}^{\ddagger}$[(Ar = $C_6H_5$) − (Ar = $C_6F_5$)] values are found to be 3.7 and 4.2 kcal/mol, respectively. See below for more discussion of the (B3LYP+D)/BS2 calculated values of the C($sp^3$)−H bond activation barriers.

The nature of each stationary point was characterized by the presence of zero or one imaginary frequency for minima and transition states, respectively. Energetics were calculated under standard conditions (1 atm and 298.15 K) and are reported as relative free energies and enthalpies in kcal/mol with the notation of $\Delta G$ ($\Delta H$). Solvent effects were accounted for in an implicit fashion using the PCM[15] formalism in toluene ($\varepsilon$ = 2.38) as in the experiments.[7] Cartesian coordinates for all reported structures are given in the Supporting Information.

## III. RESULTS AND DISCUSSION

Below, we discuss the elementary steps of the $Pd^0/PCy_3$-catalyzed *intermolecular* arylation of the terminal $\beta$-C($sp^3$)−H bond of an aryl amide (**SM** = EtCONH-Ar, where Ar = $C_6H_5$, $C_6F_5$ and CONH-Ar is a directing group (**DG**)) in the presence of CsF base.

**III.1. Oxidative Addition of Ph−I to $Pd^0/PR_3$ Catalyst.** Oxidative addition of aryl halides to $Pd^0/PCy_3$ is expected to be the initial step. Previous studies[4,5] have shown that the use of electron-rich bulky phosphine ligands facilitates oxidative addition of Ph−X by enhancing the electronegativity on the metal center and imposing coordinative unsaturation. Aryl iodides (Ph−I), which are especially reactive, are shown to undergo facile oxidative addition at room temperature.[16] Consistently, in experiments reported by Yu and co-workers[7] only aryl iodides were found to react with $Pd^0/PCy_3$ catalyst and yield the desired product.

The presented calculations show that the formation of the oxidative addition product I−$Pd^{II}$($PCy_3$)Ph (**4**) upon reacting $Pd^0/PCy_3$ (**1**) and Ph−I (**2**) is a facile process. The overall


dx.doi.org/10.1021/ja4053416 | J. Am. Chem. Soc. 2013, 135, 14206−14214

reaction **1** + **2** → **4** is exergonic ($\Delta G$ = −20.4 kcal/mol) and proceeds essentially without an energy barrier (Figure 2).

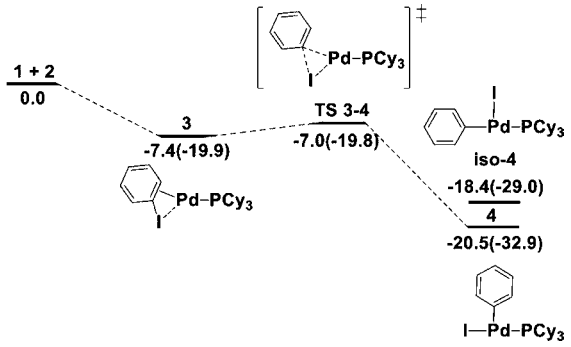


**Figure 2.** Gibbs free energy profile of the Ph−I (**2**) oxidative addition to $Pd^0/PCy_3$ (**1**). Energies are given as $\Delta G$ ($\Delta H$) in kcal/mol.

It is worth noting that the oxidative addition product $I-Pd^{II}(PCy_3)Ph$ may have another isomer, **iso-4**, which lies only 2.1 kcal/mol higher in energy than **4** (see Figure 2). Calculations show that the overall mechanisms of the arylation reaction originating from **iso-4** and **4** are the same. Furthermore, the arylation reaction originating from **iso-4** is slightly less exergonic than that for isomer **4**. Therefore, below we discuss only the mechanism of the reaction originating from **4**. Analogous intermediates, transition states, and products arising from **iso-4** are given in the Supporting Information.

**III.2. Deprotonation of Aryl Amide (SM = EtCONH−Ar) by CsF.** Deprotonation of the amide directing group of **SM**, i.e. CONH-Ar, by CsF to form **DG′** = $[EtCON\text{-}Ar]Cs^+$ is necessary for its coordination to the Pd center of the previously formed oxidative addition product **4** (Figure 3). It is worth

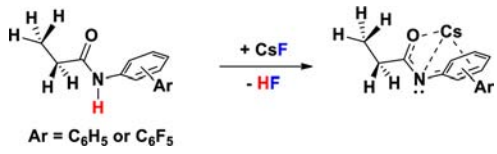


**Figure 3.** Deprotonation of the aryl amide substrate by CsF.

noting that the coordination of the imidate (**DG′**) to the Pd center minimizes the dihedral angle between C−H bonds and Pd center that facilitates the C−H bond activation.[6e]

Calculations suggest that deprotonation of **SM** by CsF is exergonic ($\Delta G$ = −24.1 and −24.8 kcal/mol for Ar = $C_6H_5$, $C_6F_5$, respectively) and proceeds with a small free energy barrier ($\Delta G^{\ddagger}$ = ∼1.6 kcal/mol). Thus, the change in acidity of the N−H bond in the amide directing group CONH-Ar by a change of the Ar component from $C_6H_5$ to $C_6F_5$ has no significant effect on the energetics of substrate deprotonation. However, the substantially lower $pK_a$ of $EtCONHC_6F_5$ (which is calculated to be approximately 6.8 units lower than that for $EtCONHC_6H_5$) is expected to shift equilibrium to the deprotonated amide species. Consequently, this would lead to the presence of a larger population of the reactive deprotonated amides for Ar = $C_6F_5$. This conclusion is supported by detailed $^1H$ NMR studies of the reactions of these two amide substrates with CsF. Indeed, in the $^1H$ NMR spectrum of the amide substrate, a broad singlet peak at 10.06 ppm was observed, which corresponds to the amide N−H peak. This peak was not observed in the spectrum of $CONHC_6F_5$/CsF mixture, and a general shift of the peaks toward higher field was observed. This experimental evidence implies that **SM** with Ar = $C_6F_5$ is indeed being deprotonated in the presence of CsF base. In contrast, the simple amide directing group $CONHC_6H_5$ remains only partially deprotonated in the presence of CsF, as the broad singlet peak (9.84 ppm), which represents amide N−H bond, does not completely disappear in the $CONHC_6H_5$/CsF mixture. The NMR spectra supporting these findings and additional experimental details have been placed in the Supporting Information.

It is important to point out that after deprotonation of **SM** by CsF and consequent removal of FH the $Cs^+$ counterion stays weakly coordinated in **DG′** = $[EtCON\text{-}Ar]Cs^+$ to the $\pi$-electronic density of its OCN-Ar directing group. The performed population analysis suggests a slight increase in negative charge on the carbonyl oxygen atom (O = −0.70 e with Cs and O = −0.65 e without Cs) upon coordination of the Cs cation. Below, we will discuss the role of the coordinated Cs cation in the following $\beta$-C($sp^3$)−H bond activation step in more detail.

**III.3. Terminal $\beta$-C($sp^3$)−H Bond Activation.** For simplicity, in this section and in section III.4, we mainly discuss the mechanistic aspects of (a) the $\beta$-C($sp^3$)−H bond activation and (b) the C($sp^3$)−Ph coupling based on the substrate with the group Ar = $C_6H_5$.

The first step of this process is the coordination of **DG′** = $[EtCON\text{-}Ar]Cs^+$ to **4**, which could occur via either a $\kappa^1$O or $\kappa^1$N center, leading to the formation of the intermediates **5a**,**b**, respectively. The geometries of the intermediates **5a**,**b** are given in Figure 4. Calculations show that the formation of **5a** is 8.1 kcal/mol less exergonic ($\Delta G$ = −13.3 kcal/mol) than the formation of **5b** ($\Delta G$ = −21.4 kcal/mol).

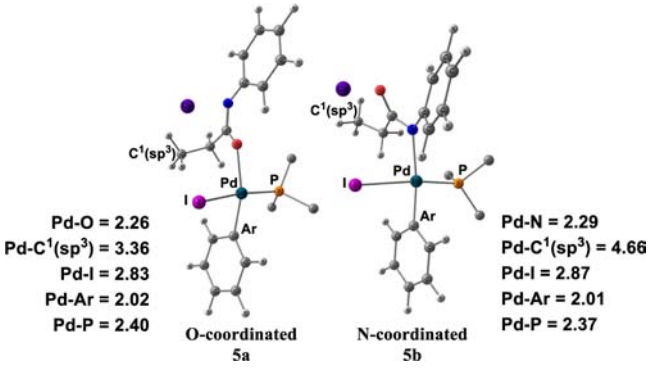


**Figure 4.** Optimized important geometries of adducts **5a**,**b**. For clarity, $PCy_3$ ligands are presented as $PC_3$. Bond lengths are given in Å.

Furthermore, the reactions initiated from **5a** proceed via the same patterns as those started from the energetically more stable isomer **5b** and are energetically less favorable (see the Supporting Information). Therefore, below we report only the reactions initiated from the intermediate **5b**.

The next step of the reaction is the C($sp^3$)−H activation of **DG′** within intermediate **5b**, which could proceed via several pathways (see Scheme 2).

*III.3.A. Oxidative Addition or "Direct-I" Assisted Deprotonation Pathways.* Classic C−H oxidative addition (which we dubbed the P-side pathway) proceeds via transition state **TS 5b-6a** and forms the intermediate **6a** with a Pd−H bond, where the H ligand is trans to the I ligand (see Figure 5). This process requires a large activation barrier of $\Delta G^{\ddagger}$ = 49.1 kcal/mol.


dx.doi.org/10.1021/ja4053416 | J. Am. Chem. Soc. 2013, 135, 14206−14214

**Scheme 2. Possible $\beta$-C(sp$^3$)−H Activation Pathways from Intermediate 5b: C−H Oxidative Addition via P-Side (Green), Direct-I Assisted C−H Activation (Orange), and Direct-F Assisted C−H Activation and $Cs_2$−I−F Cluster Assisted C−H Activation (Black) Pathways**

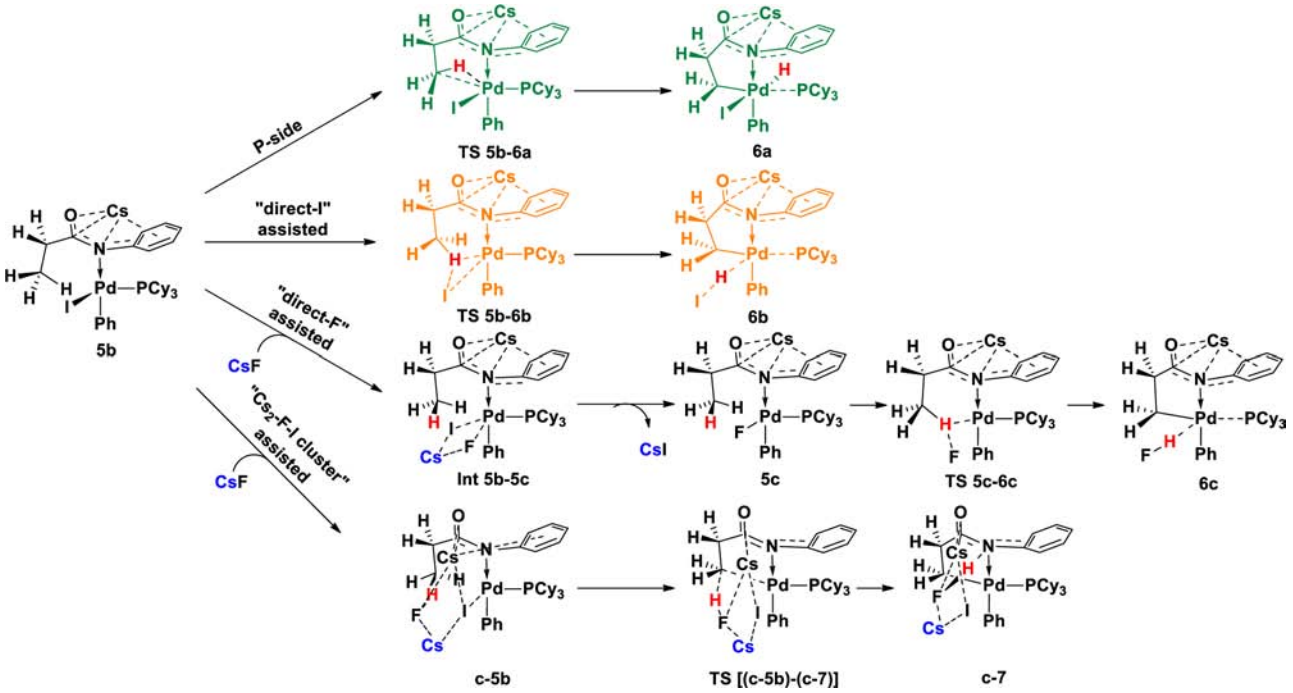


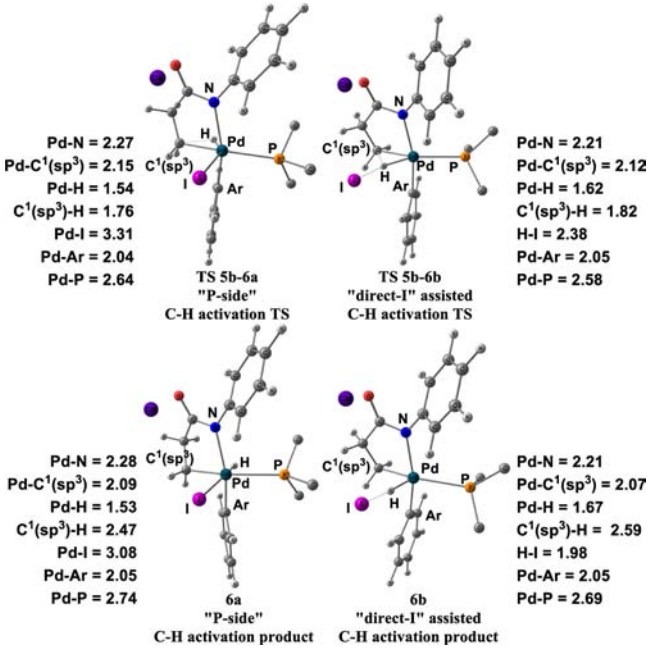


**Figure 5.** Optimized important geometries of P-side and direct-I assisted C(sp$^3$)−H bond activation transition states and the respective products. For clarity, $PCy_3$ ligands are presented as $PC_3$. Bond lengths are given in Å.

An alternative pathway, dubbed the direct-I assisted pathway, proceeds via H insertion into the Pd−I bond and concomitant formation of the Pd−C bond. This pathway proceeds through a 44.1 kcal/mol free energy barrier at transition state **TS 5b-6b** and leads to product **6b**. In other words, the direct-I assisted C(sp$^3$)−H bond activation requires ∼5 kcal/mol less energy in comparison to the P-side pathway. However, the $\beta$-C(sp$^3$)−H bond activation through both oxidative addition and direct-I assisted pathways is still high (>40 kcal/mol) in energy. Therefore, it is unlikely that the reaction outlined in Scheme 1 will proceed through these pathways.

Thus, the question remains: what is the operative mechanism of this reaction? Since experiments[7] show that CsF base facilitates this reaction, we set out to explore the effect of the CsF base on the $\beta$-C(sp$^3$)−H bond activation, at the next stage. For this reason, at first, we studied the CsF-mediated I-to-F ligand substitution in intermediate **5b** followed by direct-F assisted C−H bond activation (instead of the direct-I assisted pathway).

*III.3.B. CsF-Mediated I-to-F Substitution and Following Direct-F Assisted $\beta$-C(sp$^3$)−H Activation and Competing C(sp$^3$)−Ph Coupling Reactions.* The first step of this mechanism is the CsF-mediated I-to-F substitution in **5b** (i.e., **5b** → **5c** transformation; eq 1). Calculations show that this

$$L_nPd{-}I + CsF \rightarrow L_nPd{-}F + CsI \qquad (1)$$

reaction is thermodynamically highly favorable: $\Delta G$ = −32.9 kcal/mol (Figure 6). However, we were unable to locate the transition state associated with this substitution process for Ar = $C_6H_5$; instead, the related important intermediate (i.e.,

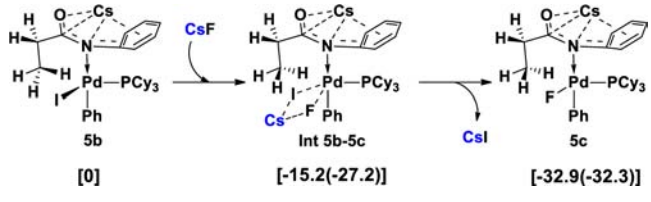


**Figure 6.** CsF-mediated I-to-F substitution assisted by $Cs^+$. Energies, $\Delta G$ ($\Delta H$), are given in kcal/mol.


dx.doi.org/10.1021/ja4053416 | J. Am. Chem. Soc. 2013, 135, 14206−14214

pretransition state structure) **Int 5b-5c** was located, which lies 15.2 kcal/mol below the reactants. Luckily, we were able to locate the transition state for the I-to-F substitution for Ar = $C_6F_5$, which is indeed relatively small: $\Delta G^{\ddagger}$ = 9.7 kcal/mol (see the Supporting Information for more details).

Thus, this finding allows us to conclude the barrier of the CsF-mediated I-to-F substitution to be small and not rate determining.

The findings presented above clearly indicate that the $Pd^{II}$–F bond is stronger than the $Pd^{II}$–I bond for this $Pd^{II}$ coordination environment. Note that NBO analysis suggests the Pd–F bond is more ionic in nature than the Pd–I bond (see the Supporting Information for more details). A similar explanation was proposed by Sakaki et al.[17] and Yates et al.[18] in a study on the role of fluoride anion in the transmetalation between vinylsilane and a $Pd^{II}$–vinyl complex and in the Stille cross-coupling reaction of Ph–Cl catalyzed by $Pd(P^tBu_3)_2$, respectively. Furthermore, recently Sanford et al. have reported experiments on a $Pd^{II}$-mediated I-to-F substitution reaction with AgF.[19]

One should note that these findings contradict the hard/soft interaction scheme, suggesting the Pd–I bond to be stronger than the Pd–F bond.[20,21] Here, it should be pointed out that the bonding environment and mechanism for direct arylation reactions, such as that presented above, are vastly different from a traditional cross-coupling scenarios. To further elaborate the Pd–halide bond strength, we also calculated the I-to-Cl and I-to-Br substitution. These calculations show that the substitution of I by Cl and Br is also favorable by $\Delta G$ = −5.8 and −1.5 kcal/mol, respectively. Thus, the stability of the $L_nPd^{II}$–X bonds is reduced in the order X = F ≫ Cl > Br > I.

The next step of the direct-F assisted pathway is the $\beta$-C($sp^3$)–H bond activation in **5c**. As seen in Figure 7, the

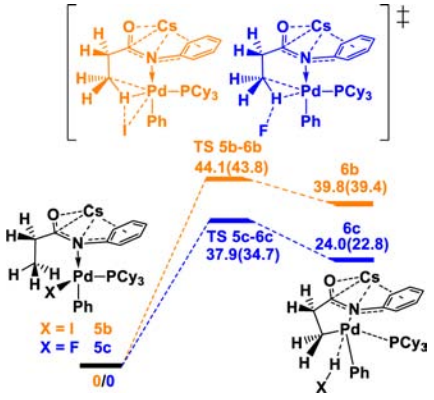


**Figure 7.** Halide identity effect in the direct-halide assisted $\beta$-C($sp^3$)–H bond activation in X–$Pd^{II}(PCy_3)$Ph(EtCON-$C_6H_5$], where X = I (**5b**), F (**5c**). Energies, $\Delta G$ ($\Delta H$), are given in kcal/mol.

product of this step, **6c**, lies only 24.0 kcal/mol higher in energy than reactant **5c**, while the product of the direct-I assisted C–H activation, **6b**, reported above, lies 39.8 kcal/mol higher than reactant **5b**. Furthermore, the calculated direct-F assisted C–H activation barrier (37.9 kcal/mol) is 6.2 kcal/mol smaller than that required for the direct-I assisted process (44.1 kcal/mol). Thus, the direct-F assisted $\beta$-C($sp^3$)–H bond activation in **5c** is kinetically and thermodynamically less demanding than the direct-I assisted C–H bond activation in **5b**.

A comparison of the computed geometries of the direct-I assisted C–H activation transition state **TS 5b-6b** (see Figure 4) and the direct-F assisted C–H activation transition state **TS 5c-6c** (see Figure 8) shows that they are fairly different. Indeed, the direct-I assisted C–H activation transition state **TS 5b-6b** can be described as an H atom insertion into the Pd–I bond mediated by the Pd center (Pd–H ≈ 1.62 Å). However, the direct-F assisted C–H activation transition state **TS 5c-6c** is closer to a direct proton abstraction without involvement ofthe Pd center (the calculated Pd–H distance is ∼2.07 Å).

Furthermore, a close examination of the geometries of the transition states **TS 5b-6a**, **TS 5b-6b**, and **TS 5c-6c** and related products **6a–c**, respectively, show that upon C–H activation the Pd–P bond elongates but *does not dissociate* (see Figures 5 and 8). This effect is more pronounced in the P-side and direct-I assisted transformations in comparison to the direct-F assisted transformations.

Although the kinetically and thermodynamically favorable CsF-mediated I-to-F substitution, i.e. eq 1, reduces the direct-halide assisted $\beta$-C($sp^3$)–H bond activation barrier, it also makes a competing Ph–F bond formation reaction possible. The calculated barrier for the Ph–F reductive elimination is found to be 23.8 kcal/mol: i.e., ca. 14 kcal/mol lower in energy in comparison to the direct-F assisted C–H bond activation. However, the Ph–F bond formation was not observed experimentally.[7] To resolve this discrepancy between the calculated and observed results, we continued to explore alternative $\beta$-C($sp^3$)–H bond activation pathways.

*III.3.C. $Cs_2$–I–F Cluster Assisted $\beta$-C($sp^3$)–H Activation Pathway.* Gratifyingly, an IRC calculation from the direct-F assisted transition state **TS 5c-6c** reveals that the F atom may never coordinate to the Pd center and may remain coordinated to the Cs center ($Cs^1$ in Figure 10). Therefore, we explored the possibility of terminal $\beta$-C($sp^3$)–H bond activation by CsF *prior* to the I-to-F substitution. Energies of the structures involved in an external (or second) CsF molecule initiated $\beta$-C($sp^3$)–H bond activation are given in Figure 9 for Ar = $C_6H_5$. The corresponding energetics for Ar = $C_6F_5$ are given in the Supporting Information.

As seen in Figure 9, upon approach of CsF to the active site (circled in Figure 9) of intermediate **5b** a $Cs_2$–I–F cluster is formed, **c-5b** (see box **a** for a general structure of this cluster). At the next stage, the formed $Cs_2$–I–F cluster abstracts a proton from the terminal methyl group at the transition state **TS**[(**c-5b**)-(**c-7**)] via its F atom. The free energy barrier at this transition state is calculated to be $\Delta G^{\ddagger}$ = 6.5. Inclusion of dispersion corrections increases it to $\Delta G^{\ddagger}_{disp}$ = 8.7 kcal/mol. Overcoming this barrier leads to formation of a diamond-shaped $Cs_2$–I–FH cluster complex, **c-7** (see box **b** for a structure of this cluster in the complex).

The optimized geometries of **c-5b**, **TS**[(**c-5b**)-(**c-7**)], and **c-7**, given in Figure 10, reveal several key points. In **c-5b**, the Pd–I bond is still intact (Pd–I = 2.91 Å) and the F atom of CsF is weakly interacting with a terminal methyl hydrogen atom (F–H(Me) = 1.91 Å). It is worth noting that both Cs atoms are interacting with the halide atoms; the calculated F–$Cs^1$/F–$Cs^2$ and I–$Cs^1$/I–$Cs^2$ bond lengths are 2.83/2.85 and 3.84/3.99 Å, respectively. Thus, in **c-5b**, the Cs cations and F and I anions form a $Cs_2$–I–F cluster. In **TS**[(**c-5b**)-(**c-7**)] the F atom is not coordinated to the Pd center (Pd–F = 2.70 Å), similar to the case for **TS 5b-5c**, and is weakly bound to the $Cs^1$ ($Cs^1$–F = 3.13 Å). Furthermore, in **TS**[(**c-5b**)-(**c-7**)] the iodide ligand is dissociating, as a part of the $Cs_2$–I–F cluster (presumably assisted by a cesium cation), and the $Cs_2$–I–(F–H) (i.e., with the F–H bond) and Pd–C bonds (Pd–C = 2.42 Å) are forming. In the product **c-7**, the newly formed $Cs_2$–I–(F–H)


dx.doi.org/10.1021/ja4053416 | J. Am. Chem. Soc. 2013, 135, 14206–14214

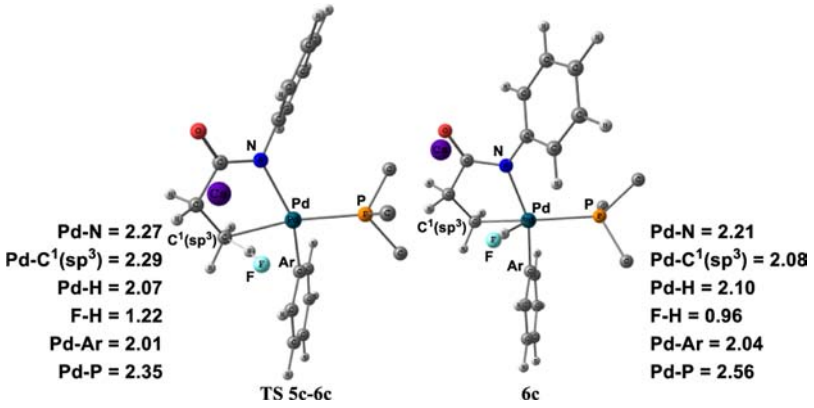


**Figure 8.** Optimized geometries of the direct-F assisted C−H bond activation transition state and the respective product. For clarity, $PCy_3$ ligands are presented as $PC_3$. Bond lengths are given in Å.

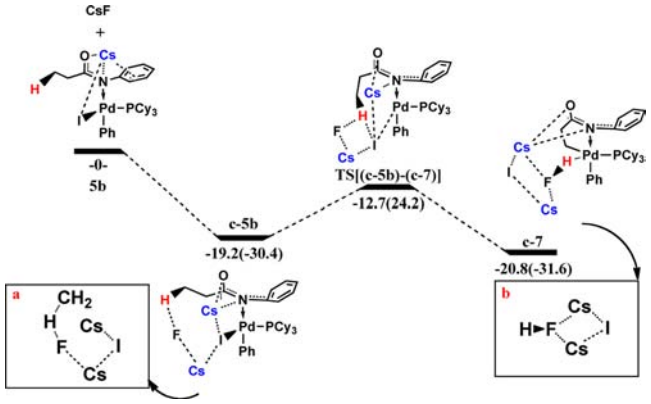


**Figure 9.** $Cs_2$−I−F cluster assisted C−H activation pathway in lieu of I-to-F substitution. Energies, $\Delta G$ ($\Delta H$), are given with respect to **5b** in kcal/mol.

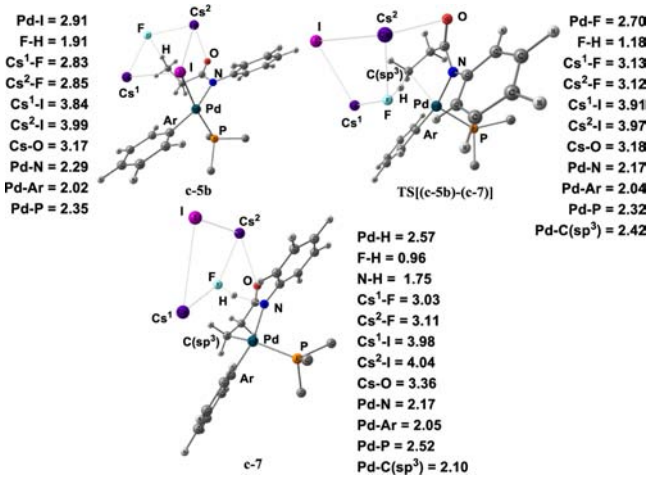


**Figure 10.** Optimized geometries of intermediates **c-5b** and **c-7** and the $Cs_2$−I−F cluster assisted hydrogen atom abstraction transition state **TS**[(**c-5b**)-(**c-7**)]. For clarity, $PCy_3$ ligands are presented as $PC_3$. Bond lengths are given in Å.

fragment is hydrogen-bonded to the nitrogen atom of the aryl amide ligand (F−H- - -*N* = 1.75 Å).

In summary, calculations convincingly show that addition of the second CsF molecule to **5b** leads to formation of a weakly coordinated $Cs_2$−I−F cluster that facilitates the abstraction of an H atom from the terminal methyl. One should note that the coordination of the $Cs_2$−I−F cluster to the Pd center by its I end, as it is in **TS**[(**c-5b**)-(**c-7**)] and (**c-7**), inhibits the Ph-F bond formation pathway.

On the basis of the findings presented above, we conclude the following. (a) The terminal $\beta$-C($sp^3$)−H bond activation of the aryl amide substrate (**SM** = EtCONH-Ar) in the presence of CsF is a facile process, requiring only a few kcal/mol of energy and proceeding via the unprecedented $Cs_2$−I−F cluster assisted mechanism. The F atom of the $Cs_2$−I−F cluster is responsible for the metalation−deprotonation process. This is the first reported example in the literature, to our knowledge, of Cs−halide cluster-mediated C−H bond activation. (b) The CsF-mediated I-to-F substitution in I−[$Pd^{II}$](Ph)($PCy_3$)(DG′) (**5b**) is a fast process, making the direct-halide assisted $\beta$-C($sp^3$)−H bond activation relatively less energetically demanding (i.e., direct-F assisted C−H activation requires a few kcal/mol less energy than the analogous direct-I assisted process) and opening up the possibility for a facile competing Ph−F bond formation reaction. (c) The direct-I assisted C−H bond activation TS is an H-atom insertion transition state into the Pd−I bond, while the direct-F assisted C−H bond activation TS is a direct proton abstraction transition state. (d) In the course of this reaction, the $PCy_3$ ligand only semidissociates.

On the basis of the aforementioned findings we should expect a dramatic effect of solvent on the mechanism of the studied reaction. Indeed, in polar solvent, where the $Cs_2$−I−F cluster is expected to completely dismantle, this reaction may proceed via the most energy demanding direct-F assisted pathway rather than the less energy demanding and unprecedented $Cs_2$−I−F cluster assisted pathway. In other words, in polar solvent this reaction either may require much harsher experimental conditions (for example much higher temperature, etc.) or may not proceed at all. This conclusion is in good agreement with our experimental findings in DMF, $^t$BuOH, and other polar solvents, which showed poor yields.

**III.4. C($sp^3$)−Ph Coupling.** Dissociation of HF and CsI molecules from the product of the most favorable $Cs_2$−I−F cluster mediated $\beta$-C($sp^3$)−H bond activation pathway, i.e. **c-7**, requires $\Delta G_{dis}$ = 14.0 kcal/mol and leads to formation of the pseudo-square-planar complex **7** (see Figure 11). The C($sp^3$)−Ph coupling is expected to start from the intermediate **7**.

Calculations show that this process requires a prohibitively high (ca. over 50 kcal/mol) energy barrier. Gratifyingly, the same process, i.e. C($sp^3$)−Ph coupling, is a facile process after the protonation of the N center of **DG′** group in **7**, i.e. from


dx.doi.org/10.1021/ja4053416 | J. Am. Chem. Soc. 2013, 135, 14206−14214

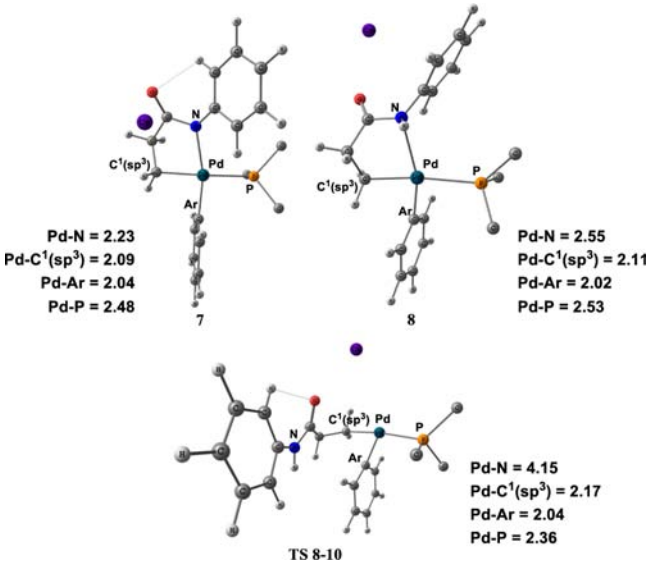


**Figure 11.** Optimized geometries of intermediates **7** and **8** and reductive elimination transition state **TS 8-10**. For clarity, $PCy_3$ ligands are presented as $PC_3$. Bond lengths are given in Å.

intermediate **8**: the associated barrier is found to be only 8.6 kcal/mol at the transition state **TS 8-10**. Formation of the product **10** with the C($sp^3$)−Ph bond is exergonic by 69.6 kcal/mol relative to **5b**. Further dissociation of the product **11** from the complex **10** costs only 9.7 kcal/mol (see Figure 12). The source of protonation of **7** is likely to be $H_2O$ from the reaction solution. Indeed, protonation of the N atom of the **DG′** group in **7** with a $(H_3O^+)(H_2O)_3$ cluster was computed to be exergonic by 24.9 kcal/mol.

In summary, reprotonation of the N center of **DG′** is essential for the C($sp^3$)−Ph cross-coupling (i.e., reductive elimination) from the product (i.e., **7**) of the most favorable $Cs_2$−I−F cluster mediated pathway. Overall, the C($sp^3$)−Ph cross-coupling from **7** is a kinetically and thermodynamically favorable process (Figure 12).

**III.5. Mechanistic Impact of the Fluorine Substitution in the Ar Group of the Substrate SM = EtCONH-Ar: Ar = $C_6H_5$ to $C_6F_5$ Substitution Effect.** The discussion presented above on the mechanism of (a) the $\beta$-C($sp^3$)−H bond activation and (b) the C($sp^3$)−Ph coupling was mainly based on the substrate with the group Ar = $C_6H_5$. However, experiments[7] show that the substrate with the group Ar = $C_6F_5$ is more reactive. In order to elucidate the role of Ar = $C_6H_5$-to-$C_6F_5$ substitution in the substrate, we calculated the full potential energy surface of the reaction for Ar = $C_6F_5$ and compared our new findings to those for Ar = $C_6H_5$ (Figure 12, see also the Supporting Information for more details). As seen from Figure 12, upon the Ar = $C_6H_5$-to-$C_6F_5$ substitution the following occurs.

(1) The $Cs_2$−I−F cluster assisted $\beta$-C($sp^3$)−H bond activation barrier is increased to $\Delta G^{\ddagger}$ = 10.2 ($\Delta G^{\ddagger}_{disp}$ = 12.9) kcal/mol (from $\Delta G^{\ddagger}$ = 6.5 ($\Delta G^{\ddagger}_{disp}$ = 8.7) kcal/mol). In other words, the Ar = $C_6H_5$-to-$C_6F_5$ substitution increases the C−H activation barrier by $\Delta G^{\ddagger}$ = 3.7 ($\Delta G^{\ddagger}_{disp}$ = 4.2) kcal/mol. However, the presence of a large population of deprotonated amide for Ar = $C_6F_5$, in comparison to that for Ar = $C_6F_5$ (see section III.2) makes the EtCONH-$C_6F_5$ a more productive substrate, as the nondeprotonated amide has a poor affinity for the $Pd^{II}$ center.

(2) The direct-F assisted $\beta$-C($sp^3$)−H activation barrier is decreased by 4.2 kcal/mol.

(3) Dissociation of HF + CsI from the **c-7** intermediate becomes 5.0 kcal/mol less endergonic.

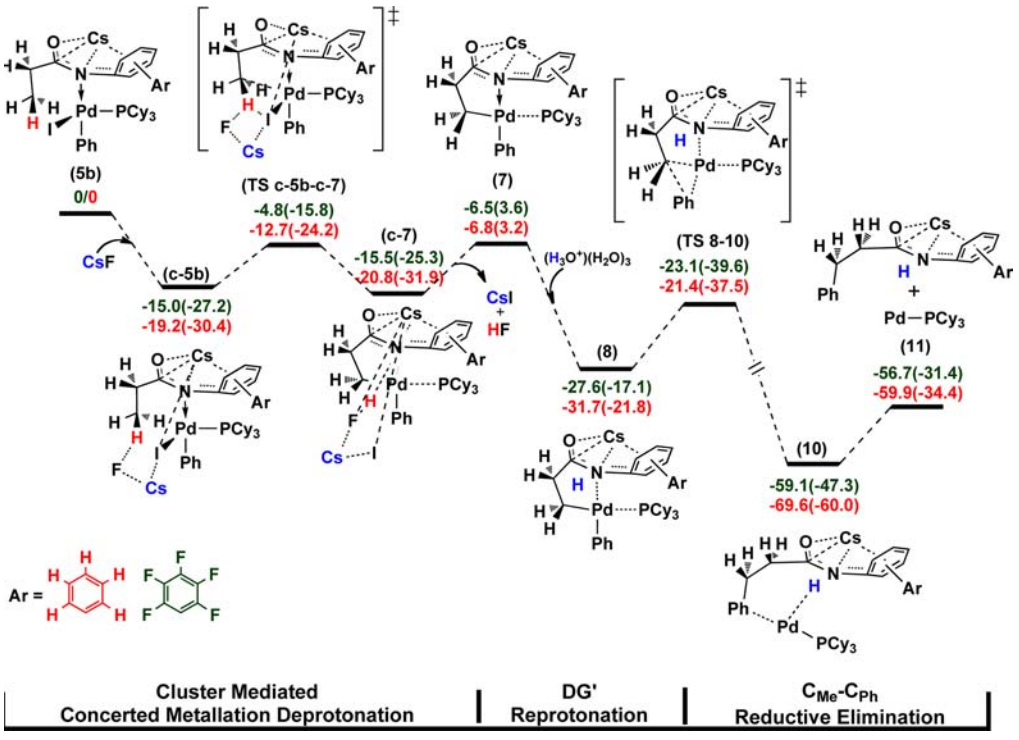


**Figure 12.** Proposed catalytic cycle for the arylation of methyl C($sp^3$)−H bonds altering the aryl component of the amide substrate for X = $C_6H_5$ (second line, red), $C_6F_5$ (first line, black). Energies, $\Delta G$ ($\Delta H$), are with respect to **5b** and are given in kcal/mol.


dx.doi.org/10.1021/ja4053416 | J. Am. Chem. Soc. 2013, 135, 14206−14214

(4) Reprotonation of the amide ligand by a hydrated $H_2O$ molecule (i.e., $(H_3O^+)(H_2O)_3$ cluster) becomes 3.8 kcal/mol more endergonic.

(5) Formation of the product **10** with a C($sp^3$)−Ph bond (i.e., **8** → **10**) becomes approximately 6.4 kcal/mol less exergonic. This is likely due to the fact that an electron-withdrawing group (such as $C_6F_5$) coordinated to the N center pushes the hybridization toward a N($sp^2$) center and weakens the coordination to the Pd center (relative to N($sp^3$)). For the same reason, the dissociation of product from **10** requires 7.3 kcal/mol less energy. Thus, the Ar = $C_6H_5$-to-$C_6F_5$ substitution makes the PES of the reaction slightly flatter and reductive elimination step slightly more favorable.

## IV. CONCLUSIONS

Mechanistic details pertaining to the $Pd^0/PCy_3$ catalyzed intermolecular arylation of the terminal $\beta$-C($sp^3$)−H bond of aryl amide (**SM** = EtCONH-Ar, where Ar = $C_6H_5$, $C_6F_5$) in the presence of CsF base have been elucidated.

Key mechanistic features of this reaction are (1) oxidative addition of aryl halide, PhI, to $Pd^0/PCy_3$, (2) deprotonation of **SM** by CsF to form imidate, **DG′** = [EtCON-Ar]$Cs^+$, for subsequent coordination to the previously formed oxidative addition product I−$Pd^{II}(PCy_3)$Ph (the substantially lower p$K_a$ of $EtCONHC_6F_5$ in comparison to $EtCONHC_6H_5$ is instrumental for the presence of a larger population of the reactive deprotonated amides for Ar = $C_6F_5$), (3) $Cs_2$−I−F cluster formation upon external (the second) CsF molecule approach to the active site of the I−$Pd^{II}(PCy_3)$Ph(DG′) intermediate, (4) $Cs_2$−I−F cluster assisted $\beta$-C($sp^3$)−H bond deprotonation by its F ligand (furthermore, the $PCy_3$ ligand only semidissociates upon the C−H bond cleavage), and (5) reprotonation of the amide directing group facilitating the C($sp^3$)−Ph reductive elimination.

We found that the CsF-mediated I-to-F substitution in I−[$Pd^{II}$](Ph)($PCy_3$)(DG′) (**5b**) is a facile process and makes the direct-halide assisted $\beta$-C($sp^3$)−H bond activation relatively less energetically demanding (i.e., direct-F assisted C−H activation requires a smaller free energy barrier than the analogous direct-I assisted process), opening the possibility for a facile competing Ph−F bond formation reaction. However, both direct-I and direct-F assisted C−H bond activation pathways require a relatively large energy barrier in comparison to the $Cs_2$−I−F cluster mediated pathway. It was shown that the direct-I assisted C−H bond activation TS is a H atom insertion transition state into the Pd−I bond, while the direct-F assisted C−H bond activation TS is a direct proton abstraction transition state with relatively low energy barrier (but still is much larger than that required for the $Cs_2$−I−F cluster assisted pathway).

## ■ ASSOCIATED CONTENT

### Supporting Information

Figures, text, and tables giving (1) a comparison of the potential energy surfaces of the reaction initiated from the $\kappa^1$O- and $\kappa^1$N-coordinated intermediates **5a**,**b**, respectively, (2) a comparison of the potential energy surfaces of the reaction initiated from oxidative addition product isomers **4** and **iso-4**, (3) effect of the F substitution in the Ar group (i.e., Ar = $C_6H_5$-to-$C_6F_5$ substitution) of **DG′** = EtCON-Ar on the direct-F assisted C−H bond activation, (4) additional information on charge analysis of [(EtCON-$C_6F_5$)$Pd^I$(Ph)($PCy_3$)]Cs and [(EtCON-$C_6F_5$)Pd(F)(Ph)($PCy_3$)]Cs complexes, (5) major competing pathways for C($sp^3$)−H bond arylation, including the I-to-F substitution and subsequent direct-F assisted C−H activation, Ph−F reductive elimination, and the $Cs_2$−I−F cluster mediated C−H activation, (6) basis sets and dispersion correction effects on the C−H bond activation, (7) $^1$H NMR and $^{19}$F NMR spectra in DMSO for the Ar = $C_6H_5$, $C_6F_5$ amide substrate treated with CsF in *d*-toluene, (8) a statement on protonation, and (9) Cartesian coordinates of all calculated species. This material is available free of charge via the Internet at http://pubs.acs.org.

## ■ AUTHOR INFORMATION


### Corresponding Authors

yu200@scripps.edu.

dmusaev@emory.edu.


### Notes

The authors declare no competing financial interest.

## ■ ACKNOWLEDGMENTS

We acknowledge the NSF Center of Chemical Innovation in Stereoselective C−H Functionalization (CHE-1205646). We also acknowledge a NSF MRI-R2 grant (CHE-0958205) and the Cherry Emerson Center for Scientific Computation.

## ■ REFERENCES


(1) For reviews on C−H activation, see: (a) Bergman, R. G. *Nature* **2007**, *446*, 391−393. (b) Labinger, J. A.; Bercaw, J. E. *Nature* **2002**, *417*, 507−514. (c) Jia, C.; Kitamura, T.; Fujiwara, Y. *Acc. Chem. Res.* **2001**, *34*, 633−639. (d) Stahl, S. S.; Labinger, J. A.; Bercaw, J. E. *Angew. Chem., Int. Ed.* **1998**, *37*, 2180−2192. (e) Shilov, A. E.; Shul'pin, G. B. *Chem. Rev.* **1997**, *97*, 2879−2932.

(2) (a) Chen, X.; Engle, K. M.; Wang, D.−H.; Yu, J.-Q. *Angew. Chem., Int. Ed.* **2009**, *48*, 5094. (b) Engle, K. M.; Mei, T.-S.; Wasa, M.; Yu, J.-Q. *Acc. Chem. Res.* **2012**, *45*, 788.

(3) (a) Neufeldt, S. R.; Sanford, M. S. *Acc. Chem. Res.* **2012**, *45*, 936−946. (b) Daugulis, O. *Top. Curr. Chem.* **2010**, *292*, 57.

(4) (a) Dyker, G. *Angew. Chem., Int. Ed.* **1992**, *31*, 1023. (b) Baudoin, O.; Herrbach, A.; Guéritte, F. *Angew. Chem., Int. Ed.* **2003**, *42*, 5736. (c) Zhao, J.; Campo, M.; Larock, R. C. *Angew. Chem., Int. Ed.* **2005**, *44*, 1873. (d) Barder, T. E.; Walker, S. D.; Martinelli, J. R.; Buchwald, S. L. *J. Am. Chem. Soc.* **2005**, *127*, 4685. (e) Ren, H.; Knochel, P. *Angew. Chem., Int. Ed.* **2006**, *45*, 3462. (f) Lafrance, M.; Gorelsky, S. I.; Fagnou, K. *J. Am. Chem. Soc.* **2007**, *129*, 14570. (g) Watanabe, T.; Oishi, S.; Fujii, N.; Ohno, H. *Org. Lett.* **2008**, *10*, 1759.

(5) For recent reviews on direct arylation, see: (a) Campeau, L. C.; Fagnou, K. *Chem. Commun.* **2006**, 1253. (b) Alberico, D.; Scott, M. E.; Lautens, M. *Chem. Rev.* **2007**, *107*, 174. (c) McGlacken, G. P.; Bateman, L. M. *Chem. Soc. Rev.* **2009**, *38*, 2447. (d) Bellina, F.; Rossi, R. *Tetrahedron* **2009**, *65*, 10269. (e) Ackermann, L.; Vicente, R.; Kapdi, A. R. *Angew. Chem., Int. Ed.* **2009**, *48*, 9792. (f) Ackermann, L.; Vicente, R. *Top. Curr. Chem.* **2010**, *292*, 211. (g) Bouffard, J.; Itami, K. *Top. Curr. Chem.* **2010**, *292*, 231. (h) Wasa, M.; Engle, K. M.; Yu, J.-Q. *Isr. J. Chem.* **2010**, *50*, 605. (i) Chuprakov, S.; Chernyak, N.; Dudnik, A. S.; Gevorgyan, V. *Org. Lett.* **2007**, *9*, 2333. (j) Seregin, I. V.; Gevorgyan, V. *Chem. Soc. Rev.* **2007**, *36*, 1173.

(6) For selected articles on directing group arylations, see: (a) Yu, J.-Q.; Giri, R.; Chen, X. *Org. Biomol. Chem.* **2006**, *4*, 4041. (b) Ryabov, A. D. *Chem. Rev.* **1990**, *90*, 403. (c) Sanford, M. S. *Top. Organomet. Chem.* **2007**, *24*, 85. (d) Ackerman, L. *Top. Organomet.Chem.* **2007**, *24*, 35. (e) Zhang, X.-G.; Dai, H.-X.; Wasa, M.; Yu, J.-Q. *J. Am. Chem. Soc.* **2012**, *134*, 11948.

(7) Wasa, M.; Engle, K. M.; Yu, J.-Q. *J. Am. Chem. Soc.* **2009**, *131*, 9886.

(8) For studies on direct arylation under ligand-free conditions, see: (a) Glover, B.; Harvey, K. A.; Liu, B.; Sharp, M. J.; Tymoschenko, M. F. *Org. Lett.* **2003**, *5*, 301. (b) Fournier, D.; Chabert, J.; Joucla, L.;

David, E.; Lemaire, M. *Tetrahedron* **2004**, *60*, 3221. (c) Parisien, M.; Valette, D.; Fangou, K. *J. Org. Chem.* **2005**, *70*, 7578. (d) Wang, X.; Gribkov, D. V.; Sames, D. *J. Org. Chem.* **2007**, *72*, 1476. (e) Tan, Y.; Hartwig, J. F. *J. Am. Chem. Soc.* **2011**, *133*, 3308.

(9) For additional studies on the role of base, see: (a) Lafrance, M.; Gorelsky, S. I.; Fagnou, K. *J. Am. Chem. Soc.* **2007**, *129*, 14570. (b) Biswas, B.; Sugimoto, M.; Sakaki, S. *Organometallics* **2000**, *19*, 3895. (c) Davies, D. L.; Donald, S. M. A.; Macgregor, S. A. *J. Am. Chem. Soc.* **2005**, *127*, 13754. (d) Davies, D. L.; Donald, S. M. A.; Al-Duaij, O.; Macgregor, S. A.; Pölleth, M. *J. Am. Chem. Soc.* **2006**, *128*, 4210. (e) Boutadla, Y.; Davies, D. L.; Macregor, S. A.; Poblador-Bahamonde, A. L. *Dalton Trans.* **2009**, 5887. (f) Garcia-Cuadrado, D.; Braga, A. A. C.; Maseras, F.; Echavarren, A. M. *J. Am. Chem. Soc.* **2006**, *128*, 1066. (g) Garcia-Cuadrado, D.; Ade Mendoza, P.; Braga, A. A. C.; Maseras, F.; Echavarren, A. M. *J. Am. Chem. Soc.* **2007**, *129*, 6880. (h) Pascual, S.; Ade Mendoza, P.; Braga, A. A. C.; Maseras, F.; Echavarren, A. M. *Tetrahedron* **2008**, *64*, 6021. (i) Lafrance, M.; Rowley, C. N.; Woo, T. K.; Fagnou, K. *J. Am. Chem. Soc.* **2006**, *128*, 8754. (j) Gorelsky, S. I.; Lapointe, D.; Fagnou, K. *J. Am. Chem. Soc.* **2008**, *130*, 10848. (k) Liégault, B.; Petrov, I.; Gorelsky, S. I.; Fagnou, K. *J. Org. Chem.* **2010**, *75*, 1047. (l) Ess, D. H.; Bischof, S. M.; Oxgaard, J.; Periana, R. A.; Goddard, W. A., III *Organometallics* **2008**, *27*, 6440. (m) Kefalidis, C. E.; Baudoin, O.; Clot, E. *Dalton Trans.* **2010**, *39*, 10528.

(10) For initial studies on CMD mechanisms, see: (a) Gomez, M.; Granell, J.; Martinez, M. *Organometallics* **1997**, *16*, 2539. (b) Gómez, M.; Granell, J.; Martinez, M. *J. Chem. Soc., Dalton Trans.* **1998**, 37.

(11) Frisch, M. J.; Trucks, G. W.; Schlegel, H. B.; Scuseria, G. E.; Robb, M. A.; Cheeseman, J. R.; Scalmani, G.; Barone, V.; Mennucci, B.; Petersson, G. A.; Nakatsuji, H.; Caricato, M.; Li, X.; Hratchian, H. P.; Izmaylov, A. F.; Bloino, J.; Zheng, G.; Sonnenberg, J. L.; Hada, M.; Ehara, M.; Toyota, K.; Fukuda, R.; Hasegawa, J.; Ishida, M.; Nakajima, T.; Honda, Y.; Kitao, O.; Nakai, H.; Vreven, T.; Montgomery, J. A., Jr.; Peralta, J. E.; Ogliaro, F.; Bearpark, M.; Heyd, J. J.; Brothers, E.; Kudin, K. N.; Staroverov, V. N.; Kobayashi, R.; Normand, J.; Raghavachari, K.; Rendell, A.; Burant, J. C.; Iyengar, S. S.; Tomasi, J.; Cossi, M.; Rega, N.; Millam, J. M.; Klene, M.; Knox, J. E.; Cross, J. B.; Bakken, V.; Adamo, C.; Jaramillo, J.; Gomperts, R.; Stratmann, R. E.; Yazyev, O.; Austin, A. J.; Cammi, R.; Pomelli, C.; Ochterski, J. W.; Martin, R. L.; Morokuma, K.; Zakrzewski, V. G.; Voth, G. A.; Salvador, P.; Dannenberg, J. J.; Dapprich, S.; Daniels, A. D.; Farkas, Ö.; Foresman, J. B.; Ortiz, J. V.; Cioslowski, J.; Fox, D. J. *Gaussian 09, Revision A1*; Gaussian, Inc., Wallingford, CT, 2009.

(12) Zhao, Y.; Truhlar, D. G. *Theor. Chem. Acc.* **2008**, *120*, 215.

(13) (a) Hay, P. J.; Wadt, W. R. *J. Chem. Phys.* **1985**, *82*, 299. (b) Hay, P. J.; Wadt, W. R. *J. Chem. Phys.* **1985**, *82*, 284. (c) Wadt, W. R.; Hay, P. J. *J. Chem. Phys.* **1997**, *107*, 3032.

(14) (a) Grimme, S. *J. Comput. Chem.* **2004**, *25*, 1463. (b) Grimme, S. *J. Comput. Chem.* **2006**, *27*, 1787. (c) Grimme, S.; Antony, J.; Ehrlich, S.; Krieg, H. *J. Chem. Phys.* **2010**, *132*, 154104.

(15) Tomasi, J.; Mennucci, B.; Cammi, R. *Chem. Rev.* **2005**, *105*, 2999.

(16) Senn, H. M.; Ziegler, T. *Organometallics* **2004**, *23*, 2980.

(17) Sugiyama, A.; Ohnishi, Y.; Nakaoka, M.; Nakao, Y.; Sato, H.; Sakaki, S.; Nakao, Y.; Hiyama, T. *J. Am. Chem. Soc.* **2008**, *130*, 12975.

(18) Ariafard, A.; Yates, B. F. *J. Am. Chem. Soc.* **2009**, *131*, 13981.

(19) Ball, N. D.; Kampf, J. W.; Sanford, M. S. *Dalton Trans.* **2010**, *39*, 632.

(20) Fagnou, K.; Lautens, M. *Angew. Chem., Int. Ed.* **2002**, *41*, 26.

(21) (a) Ananikov, V. P.; Musaev, D. G.; Morokuma, K. *Eur. J. Inorg. Chem.* **2007**, 5399. (b) Ananikov, V. P.; Musaev, D. G.; Morokuma, K. *Organometallics* **2005**, *24*, 723.